Technical Report

TR-10-31

Material model for shear of the buffer – evaluation of laboratory test results

Lennart Börgesson, Ann Dueck, Lars-Erik Johannesson
Clay Technology AB

December 2010

Svensk Kärnbränslehantering AB
Swedish Nuclear Fuel
and Waste Management Co

Box 250, SE-101 24 Stockholm
Phone +46 8 459 84 00

ISSN 1404-0344
SKB TR-10-31

Material model for shear of the buffer – evaluation of laboratory test results

Lennart Börgesson, Ann Dueck, Lars-Erik Johannesson
Clay Technology AB

December 2010

Keywords: SKBdoc 1223374, Bentonite, Buffer, Earthquake, Laboratory tests, Material model, Rate dependancy, Stress-strain relation, Shear strength.

Abstract

The report describes the material model of bentonite used for analysing a rock shear through a deposition hole. The old model used in SR-Can has been considerably changed. The new reference model that has been developed for SR-Site is described and motivated.

The relevant properties of the buffer that affect the response to a rock shear are (in addition to the bentonite type) the density (which yields a swelling pressure), the shear strength, the stiffness before the maximum shear stress is reached and the shear rate, which also affects the shear strength. Since the shear caused by an earthquake is very fast and the hydraulic conductivity of the bentonite is very low there is no possibility for the pore water in the water saturated bentonite to be redistributed. Since the compressibility of water and particles are negligible, the bentonite can be modelled as a solid material that cannot change volume but only exhibit shear deformations.

A proper and simple model that behaves accordingly is a model with von Mises' stress modelled as a function of the strain (stress-strain model). The model is elastic-plastic with an E-modulus that determines the behaviour until the material starts yielding whereupon the plastic strain is modelled as a function of von Mises' stress and added to the elastic strain. Included in the model is also a strain rate dependency of the stress-strain relation, which ranges between the strain rates 10^{-6} 1/s < ν < 10^{3} 1/s.

The reference material model is derived from a large number of laboratory tests made on different bentonites at different strain rates, densities and with different techniques. Since it cannot be excluded that the exchangeable cat-ions in the Na-bentonite MX-80 is exchanged to calcium-ions the Ca-bentonite Deponit CaN is proposed to be used as reference material.

The overall conclusion is that a relevant and probably also slightly conservative material model of Ca-converted MX-80 is derived, presented and well motivated.

Sammanfattning

I rapporten beskrivs den materialmodell för bentonit som används för att analysera en bergskjuvning genom ett deponeringshål. Den gamla modellen som användes i SR-Can har blivit avsevärt förändrad. Den nya referensmodellen som har utvecklats för SR-Site, beskrivs och motiveras.

De relevanta egenskaperna hos bufferten som har betydelse för inverkan av en bergskjuvning är (förutom bentonitens sammansättning) densiteten (som ger ett svälltryck), skjuvhållfastheten, materialets styvhet innan maxspänningar uppnåtts och skjuvhastigheten som även påverkar skjuvhållfastheten. Eftersom skjuvningen orsakad av ett jordskalv är mycket snabb och bentonitens hydrauliska konduktivitet mycket låg finns det ingen möjlighet för vattnet i den vattenmättade bentoniten att omfördelas. Eftersom kompressibiliteten hos vatten och partiklar är försumbar kan bentoniten modelleras som ett solitt material som inte kan ändra volym utan enbart förete skjuvdeformationer.

En lämplig och enkel modell som uppför sig på detta sätt är en modell med von Mises' spänning modellerad som en funktion av töjningen (spännings-töjningsmodell). Modellen är elasto-plastisk med en E-modul som styr beteendet tills materialet börjar plasticeras varefter den plastiska töjningen modelleras som en funktion av von Mises'– spänningen och adderas till den elastiska töjningen. Modellen inkluderar också ett töjningshastighetsberoende inom ett stort hastighetsintervall 10^{-6} 1/s < v < 10^{3} 1/s.

Referensmodellen är härledd ur ett stort antal laboratorieförsök som gjorts på olika bentoniter vid olika töjningshastigheter och densiteter och med olika teknik. Eftersom ett jonbyte inte kan uteslutas, där utbytbara katjoner i Na-bentoniten MX-80 byts mot kalciumjoner, föreslås Ca-bentoniten Deponit CaN användas som referensmaterial.

En generell slutsats är att en relevant och välmotiverad och troligen även något konservativ materialmodell av Ca-omvandlad MX-80 har tagits fram och presenterats.

Contents

1 Introduction

1.1 Background

This report is one in a series of reports that together address the response of the buffer and the canister in a KBS-3V repository to shear movements in a fracture intersecting deposition holes.

The report describes the material model that has been used for modeling the bentonite buffer in the analyses of the effect of a rock shear through a deposition hole. The report is meant to merge the present knowledge including the latest test results and to derive a material model that is used for the SR-Site modelling of the rock shear scenarios /Hernelind 2010/ and form the basis of the canister design analysis /Raiko et al. 2010/.

A number of tests for settling the model and for describing its relation to the important variables (mainly the density, the swelling pressure, the shear strength and the rate of strain) for different bentonites have been done and reported earlier (see e.g. /Börgesson et al. 1995, 2004/). This model is described more in detail in Chapter 2. The model has been used for calculating the stresses in the canister at different types of rock shear /Börgesson et al. 2004, Börgesson and Hernelind 2006/ and a similar model is used for calculations for SR-Site.

The material model is being verified by three model shear tests that represent a deposition hole in the scale 1:10 performed 20 years ago, which have been modelled with the material model of MX-80 adapted to the test conditions, but the calculations and the reporting were finished late /Börgesson and Hernelind 2010/ and this verification will not be further referred to.

A large number of new tests have been made in order to update the model, apply it to ion-exchanged MX-80 and include strain rate dependency. These tests are reported in a separate report /Dueck et al. 2010/.

1.2 Behaviour of the bentonite buffer during fast shear

When a fracture intersecting a deposition hole is affected by a nearby earthquake the fracture may slip and cause a shearing of the buffer and the enclosed canister. The magnitude of such a rock shear and the rate of rock shear displacement have been estimated to be at maximum 5–10 cm and 1.0 m/s respectively, which are stipulated as dimensioning values.

During a rock shear through a deposition hole, the buffer material plays an important role to cushion the stress transfer since the buffer material is much softer than both the rock and the canister. Since the stiffness and the shear strength of the buffer material is rather low the most stressed parts of the buffer close to the shear plane will plasticize and thus only transfer a small fraction of the rock displacements to the canister. However, since those properties are very sensitive to the density of the bentonite, also within the relatively small density interval accepted for the buffer material (1,950 kg/m^3 < ρ_m < 2,050 kg/m^3), the stiffness and shear strength and thus also the effect on the canister can vary substantially.

The Na-bentonite MX-80 at the target average density at water saturation 2,000 kg/m^3 has been appointed the reference buffer material. The properties of MX-80 have been investigated and reported in many projects. The relevant properties that affect the response to a rock shear are the density (which yields a swelling pressure), the shear strength, the stiffness before the maximum shear stress is reached and the shear rate, which also affects the shear strength. Since the shear is very fast and the hydraulic conductivity of the bentonite is very low there is no possibility of the pore water in the water saturated bentonite to be redistributed and since the compressibility of water and particles are negligible, the bentonite can be modelled as a solid material that cannot change volume but only exhibit shear deformations.

A proper and simple model that behaves accordingly is a model with von Mises' stress as a function of the strain (stress-strain model). The model is elastic-plastic with an E-modulus that determines the behaviour until the material starts yielding whereupon the plastic strain is modelled a function of von Mises' stress and added to the elastic strain.

All densities mentioned in this report refer to the density at full water saturation.

2 Material model used in SR-Can

This chapter gives a general description and motivation for the model of the buffer material and specific data used for the modelling of the rock shear case in SR-Can /Börgesson et al. 2004/.

2.1 General

The bentonite buffer is modelled using only total stresses that don't include the pore water pressure, the reason being the very fast compression and shear as noted in Chapter 1. The stress-strain relation is expressed with von Mises' stress σ_j that describes the "shear stress" in three dimensions according to Equation 2-1.

$$\sigma_j = (((\sigma_1 - \sigma_3)^2 + (\sigma_1 - \sigma_2)^2 + (\sigma_2 - \sigma_3)^2)/2)^{1/2} \quad (2\text{-}1)$$

where

σ_1, σ_2 and σ_3 are the major principal stresses.

At triaxial tests σ_2 and σ_3 are equal and von Mises' stress equal to the deviator stress q.

$$q = (\sigma_1 - \sigma_3) \quad (2\text{-}2)$$

The model includes an elastic part and a plastic part. The actual parameter values in the model depend very much on a number of factors that have to be settled. Equations 2-3 to 2-5 are used for defining the shear strength and the influence of density, swelling pressure and rate of shear (see /Börgesson et al. 1995, 2004/).

2.2 Relation between swelling pressure and void ratio

The relation between swelling pressure and void ratio was described according to Equation 2-3:

$$p = p_0 \left(\frac{e}{e_0} \right)^{\frac{1}{\beta}} \quad (2\text{-}3)$$

where

e = void ratio

e_0 = reference void ratio (= 1.1)

p = swelling pressure (at e)

p_0 = reference swelling pressure (at e_0) (= 1,000 kPa)

β = –0.19

The values used for e_0, p_0 and β were derived for MX-80 and the resulting relation, which is illustrated in Chapter 3, fits fairly well with new measurements. For the reference buffer material in SR-Can the swelling pressure, at the target average density at water saturation ρ_m = 2,000 kg/m^3 (e = 0.78), was according to this model

p = 6.1 MPa

2.3 Relation between shear strength and swelling pressure

The relation between shear strength (or actually deviator stress at failure) and swelling pressure was described according to Equation 2-4:

$$q_f = q_{f0}\left(\frac{p}{p_0}\right)^b \tag{2-4}$$

where

q_f = deviator stress at failure at the swelling pressure p

q_{f0} = 500 kPa (deviator stress at failure at the swelling pressure p_0)

p_0 = 1,000 kPa

b = 0.77

The parameter values were based on triaxial tests on MX-80 with the very low shear rate $v_s \approx 5 \cdot 10^{-5}$ mm/s. The new tests confirm this relation (see Chapter 3). For the reference buffer material at the target average density at water saturation ρ_m = 2,000 kg/m^3 (e = 0.78) the shear strength at the reference swelling pressure p = 6.1 MPa would according to this model be

q_f = 2.0 MPa

2.4 Relation between shear strength and shear rate

The relation between shear strength and shear rate was described according to Equation 2-5:

$$q_{fs} = q_{fs0}\left(\frac{v_s}{v_{s0}}\right)^n \tag{2-5}$$

where

v_s = shear rate (m/s)

v_{s0} = reference shear rate (m/s)

q_{fs} = deviator stress at failure at the shear rate v_s (kPa)

q_{fs0} = deviator stress at failure at the reference shear rate v_{s0} (kPa)

n = 0.065

The value n = 0.065 was found for MX-80 at low shear rates and verified by tests with shear rates up to 1 m/s although late tests and re-evaluation indicate that n is smaller, which means that the rate dependence probably is lower. For the reference buffer material at the target average density at water saturation ρ_m = 2,000 kg/m^3 the shear strength would, at the dimensioning shear rate 1 m/s be (Equation 2-5 with n = 0.065, $v_{s0} = 5 \cdot 10^{-8}$ m/s and q_{fs0} = 2.0 MPa)

q_f = 6.0 MPa

2.5 Elastic part of the stress-strain relation

Numerous triaxial and unconfined compression tests have shown that the stress-strain relation during shear is rather similar if the deviator stress (Mises stress) is normalised against the strength (maximum deviator stress). This means that both the elastic and the plastic parts are proportional to the actual strength. For the reference buffer material at the target average density at water saturation $\rho_m = 2{,}000$ kg/m^3 ($e = 0.78$) the E-modulus $E = 363$ MPa at $q_{fs} = 6{,}300$ kPa ($v_s = 1{,}000$ mm/s) was used /Börgesson et al. 2004/.

The shear takes place at such a high rate that no pore water transport can occur during the shear, which means that no volume change of the water saturated material can take place. Thus Poisson's ratio must be close to 0.5, corresponding to no volume change. However, a small amount of volume change will appear due to compressibility of water and therefore Poisson's ratio has been chosen to 0.49 in all calculations. I addition, with Poisson's ratio slightly less than 0.5, the problem is better conditioned for the numerical solver.

2.6 Elastic-plastic stress-strain relation

The plastic part of the stress-strain relation was chosen so that the maximum shear stress would occur at the strain 3%. This is lower than achieved by measurements and has been revised to 5.4% in the new model presented in Chapter 4. The material model used for the reference buffer material at the target average density at water saturation $\rho_m = 2{,}000$ kg/m^3 ($e = 0.78$) is shown in Table 2-1 and Figure 2-1. Figure 2-1 also shows the models used in SR-Can for higher density and for Ca-bentonite.

Table 2-1. Elastic-plastic material data for the bentonite buffer – MX-80 at the density at saturation 2,000 kg/m^3.

Elastic part		Plastic part: von Mises stress σ_j (MPa) at the following plastic strains (ε_p)							
E (MPa)	v	ε_p=0	ε_p=0.002	ε_p=0.005	ε_p=0.009	ε_p=0.013	ε_p=0.018	ε_p=0.023	ε_p=1.0
363	0.49	3.63	4.85	5.57	5.95	6.19	6.3	6.22	6.22

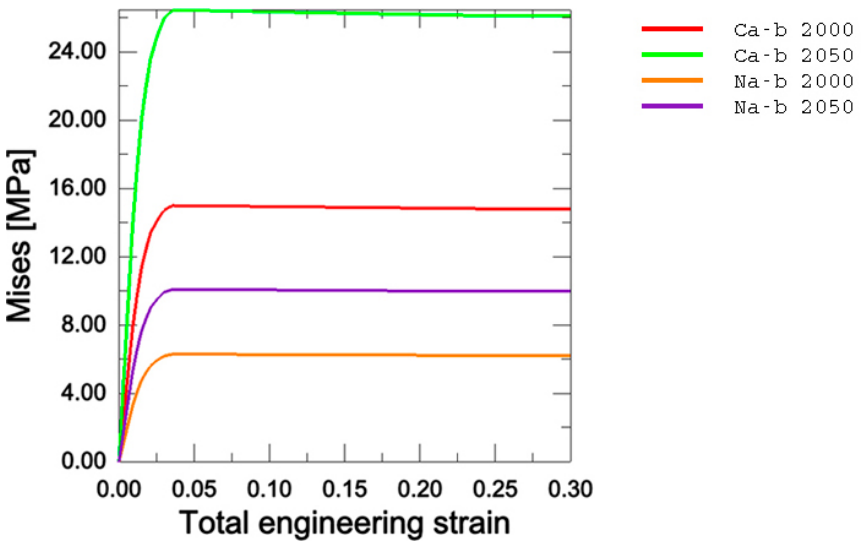

Figure 2-1. *Mises stress as function of strain for four bentonite materials at the shear rate 1 m/s. The reference material (MX-80 at the density 2,000 kg/m^3) is the lower orange line. Relations used in SR-Can.*

3 Laboratory tests

3.1 General

New measurements, which are reported in this chapter, have yielded updated models for MX-80 and for the Ca-bentonite that can be expected to be the result of an ion-exchange from Na to Ca (here called MX-80Ca).

In Chapter 2 it was shown that there are a number of relations and dependencies that contribute to the response of bentonite to fast shearing.

The most important relations are

- swelling pressure as function of the density,
- shear strength as function of the swelling pressure,
- stress-strain relation.

The most important dependencies are

- influence of shear rate,
- influence of salt content and exchangeable cat ion in the ground water,
- influence of stress history.

The reference buffer material to be installed in the deposition holes is Na-bentonite MX-80 at the average density $\rho = 2{,}000$ kg/m^3 after water saturation and homogenisation. However, acceptable limits are 1,950 kg/m^3 $< \rho <$ 2,050 kg/m^3, which means that the canister needs to withstand a rock shear at the density $\rho = 2{,}050$ kg/m^3, which yields the highest shear strength.

Since it cannot be ruled out that there will be an ion-exchange from Na to Ca and since the groundwater can have a variation in salt content these processes must be considered. Tests have been performed on MX-80 both after ion-exchange to Ca and after exposure to high salt content of NaCl in the pore water.

The tests made to investigate the shear strength and the stress-strain relation are either triaxial tests or unconfined compression tests, both of which are usually made with much slower shear rate than what corresponds to the reference shear rate 1.0 m/s. Those test results must thus be adjusted for influence of the shear rate and a large number of tests have been done with shear rates up to several meters per second.

Tests made on MX-80 exposed to very high water pressure (that may occur during a glaciation) have indicated that there is a remaining increase in swelling pressure after such a stress history /Harrington and Birchall 2007/. In order to investigate if this effect also yields increased shear strength a series of mainly triaxial tests has been performed.

Also the influence of temperature has been investigated. All tests have been performed at room temperature. In order to see if the lower temperature that is expected to prevail at a rock shear will influence the shear strength, a number of unconfined compression tests at the temperature 5–15ºC have been made.

3.2 Tests

The following tests have been performed in order to increase the knowledge of the mechanical properties of the buffer material with special emphasis on fast shearing:

- Tests of MX-80 that has been exposed to very high water pressure.
- Tests on a Ca-bentonite that resembles ion-exchanged MX-80 (Deponit CaN).
- Tests on ion-exchanged MX-80 (MX-80Ca).
- Tests on Deponit CaN at lower temperature.

The laboratory test results are in detail reported by /Dueck et al. 2010/. The results will be summarized in this report.

3.3 Results and evaluation

The results have been summarized in a number of diagrams, which for comparison also include other results.

3.3.1 Swelling pressure

The swelling pressure has been measured in connection with the triaxial tests in several ways, both in oedometers during water saturation of the test samples, in the triaxial cells before shearing and as RH-measurements of the samples after the tests. Figure 3-1 shows a compilation of the results for MX-80. Equation 2-3 with the parameter values shown in Chapter 2, which were used in SR-Can, is included in the figure.

The figure shows that the measured swelling pressures are located on a line that deviates slightly from Equation 2-3 and for void ratio $0.7 < e < 0.9$ is located slightly above Equation 2-3. Equation 3-2 thus seems to underestimate the swelling pressure with 1–2 MPa with the parameters shown in section 2.2 and used in SR-Can.

Figure 3-2 shows the same relation for Ca-bentonites, both a natural Ca-bentonite with similar chemical status as MX-80 (named Deponit CAN) and MX-80Ca, which is MX-80 that has been ion-exchanged to Ca. No obvious difference between MX-80Ca and Deponit CaN can be seen. The results fit well to the solid line representing Equation 2-3 (below renamed Equation 3-1) with the following parameter values (derived from adaption to the new test results):

$$p = p_0 \left(\frac{e}{e_0} \right)^{\frac{1}{\beta}} \qquad (3\text{-}1)$$

p = swelling pressure at the void ratio e

p_0 = 1,000 kPa

e_0 = reference void ratio (= 1.33)

b = –0.254

The *dimensioning* swelling pressure for MX-80Ca for the shear calculations at the density 2,050 kg/m^3 (e = 0.70) is thus according to Equation 3-1 p = 12.5 MPa.

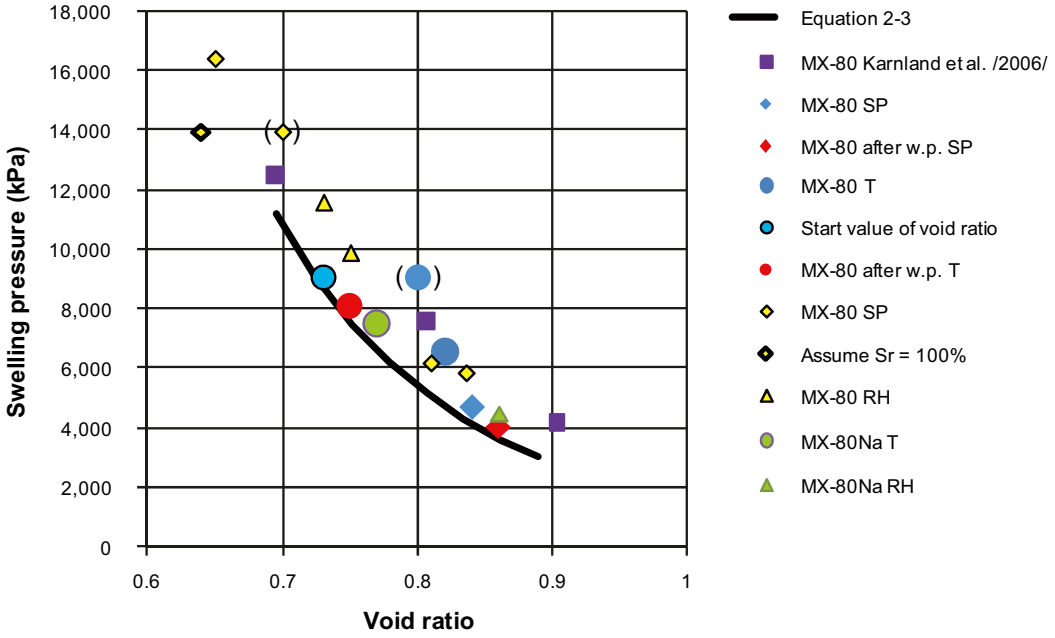

Figure 3-1. *Compilation of swelling pressure measurements made on MX-80 in the tests presented by /Dueck et al. 2010/. The solid line represents Equation 2-3 with the parameter values shown in Chapter 2.*

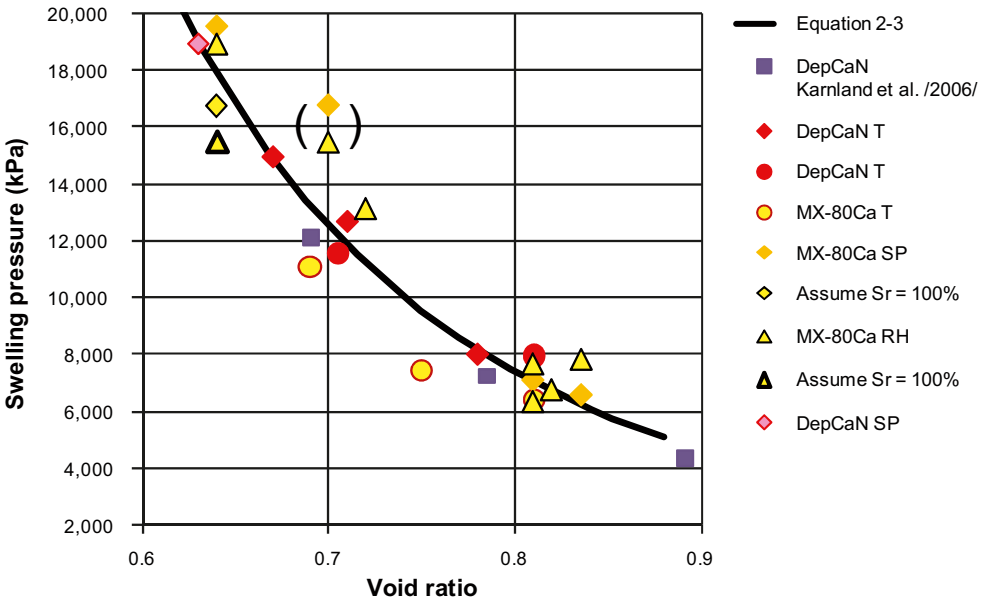

Figure 3-2. *Compilation of swelling pressure measurements made on Ca-bentonites in the tests presented by /Dueck et al. 2010/. The solid line represents Equation 2-3 with the parameter values adapted to the test results.*

3.3.2 Shear strength

The results from the triaxial tests are shown in Figure 3-3 with the deviator stress at failure plotted as function of the effective average stress (swelling pressure). Old results for MX-80 and Moosburg Ca-bentonite are also shown (non-triangles).

Figure 3-3 is plotted with the effective stress variable p', which is the total average stress p minus the pore water pressure u as described by Equations 3-2 and 3-3.

$$p' = p - u \tag{3-2}$$

$$p = (\sigma_1 + \sigma_2 + \sigma_3)/3 \tag{3-3}$$

The best fitted curves according to Equation 2-4 (renamed below as Equation 3-4) are plotted. The parameters evaluated for the different materials according Equation 3-4, are shown in Table 3-1.

$$q_f = q_{f0}\left(\frac{p}{p_0}\right)^b \tag{3-4}$$

where

q_f = deviator stress at failure at the swelling pressure p

q_{f0} = deviator stress at failure at the swelling pressure p_0

p_0 = 1,000 kPa

b = 0.77

At undrained conditions Equation 3-4 is valid for water saturated clays with a gas pressure significantly lower than the swelling pressure.

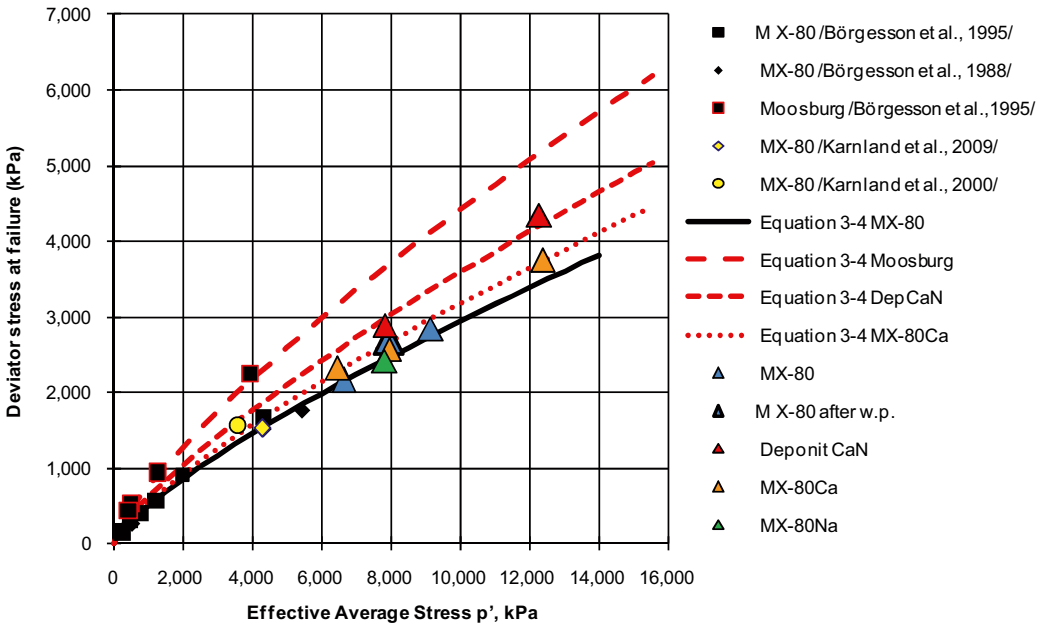

Figure 3-3. *Results from triaxial tests with the deviator stress at failure plotted as function of the effective average stress. The lines represent evaluation of Equation 3-4. See Table 3-1. The red triangles refer to Deponit CaN, the orange triangles refer to MX-80Ca, the blue triangles refer to MX-80 and the green triangle represents the test on MX-80Na. The dark blue triangle (almost hidden) at p' = 8 MPa represents the sample that had been exposed to a high water pressure. The nine new tests reported by /Dueck et al. 2010/ are marked as large triangles and made with the shear rate 0.4–0.9·10^{-8} m/s.*

Table 3-1. Parameters in Equation 3-4 evaluated from the triaxial test results shown as lines in Figure 3-3.

Material (symbol)	b	p_0 (kPa)	q_{f0} (kPa)	Reference
MX-80	0.77	1,000	500	/Börgesson et al. 1995/
Moosburg Ca	0.77	1,000	750	/Börgesson et al. 1995/
Deponit CaN	0.77	1,000	610	This report
MX-80Ca	0.77	1,000	540	This report

The validity of Equation 3-4 in the rock shear analyses is based on the important observation that the stress path in all triaxial tests is vertical in a diagram like Figure 3-3 (see e.g. /Dueck et al. 2010/), which means that the pore water pressure is balancing the increase in average total stress caused by the increase in principle stress σ_1 during shear, so that the average effective stress p' remains constant. This means that the swelling pressure can be used in Equation 3-4, since the average effective stress does not change during shear. Equation 3-4 is thus valid independent of the total stress path, which confirms that the pore water pressure is not required in the model but a total stress model and a Mises model with stress-independent strength can be used.

Figure 3-3 and Table 3-1 show the following:

The relation for MX-80 fits well with the new measurements but the triaxial test made on the sample that had been exposed to a high water pressure shows a slightly higher strength. However, the difference is small and is considered to be within the margin of natural scatter so the conclusion is that a history of high water pressure does not yield an increase in shear strength. Unconfined compression tests made on the same materials confirm these results /Dueck et al. 2010/. Also the result with MX-80 "ion exchanged" to Na (MX-80Na) and made with a 0.6 M NaCl solution (≈ 3.5% salt content) in equilibrium with the sample agrees with the results of MX-80.

The old relation for Moosburg Ca-bentonite (with q_{f0} = 750 kPa) is located high above the new measurements and it is concluded that this bentonite differ substantially from what can be expected from ion-exchanged MX-80.

The two tests on Deponit CaN yield higher strength than MX-80 but lower than Moosburg Ca and fit well with the line with q_{f0} = 610 kPa.

The three tests with ion-exchanged MX-80 (MX-80Ca) yield shear strengths (orange triangles) that are located between the relations for MX-80 and Deponit CAN and fits well to Equation 3-4 with q_{f0} = 540 kPa. One of these tests was made with the sample in equilibrium with a 0.3 M $CaCl_2$ solution (≈ 4.2% salt content).

A compilation of the results of the triaxial tests with the shear rate 4–9·10^{-6} mm/s and the unconfined compression tests with the shear rate 5·10^{-3} mm/s are shown in Figure 3-4.

Figure 3-4 shows that the evaluation of Equations 3-1 and 3-4 fits well with measured results for Deponit CaN while the relation for MX-80 logically underestimates the strength slightly due to the underestimated swelling pressure. The figure also shows that the influence of decreased temperature is insignificant and that MX-80Ca is more in agreement with the results of MX-80 than Deponit CaN.

The chosen *dimensioning* shear strength of ion-exchanged MX-80 is described by Equation 3-4 with q_{f0} = 610 kPa (corresponding to the results of Deponit CaN), which yields a deviator stress at failure of q_f = 4.27 MPa at the swelling pressure 12.5 MPa and the deformation rate ~1.0·10^{-7} m/s. The motivations for choosing this relation are the following:

- There are no other tests made on MX-80Ca than the triaxial tests due to the complicated and time-consuming process of ion exchange so there is no information on the influence of shear rate like the results shown later in Figure 3-5.
- The only test on MX-80Ca made at the density 2,050 kg/m^3 fits well into the trend for Deponit CaN as shown later in Figure 3-5.
- Since the strength of MX-80Ca measured in the triaxial tests is lower than the corresponding strength of Deponit CaN a choice of Depoint CaN as reference is slightly conservative.

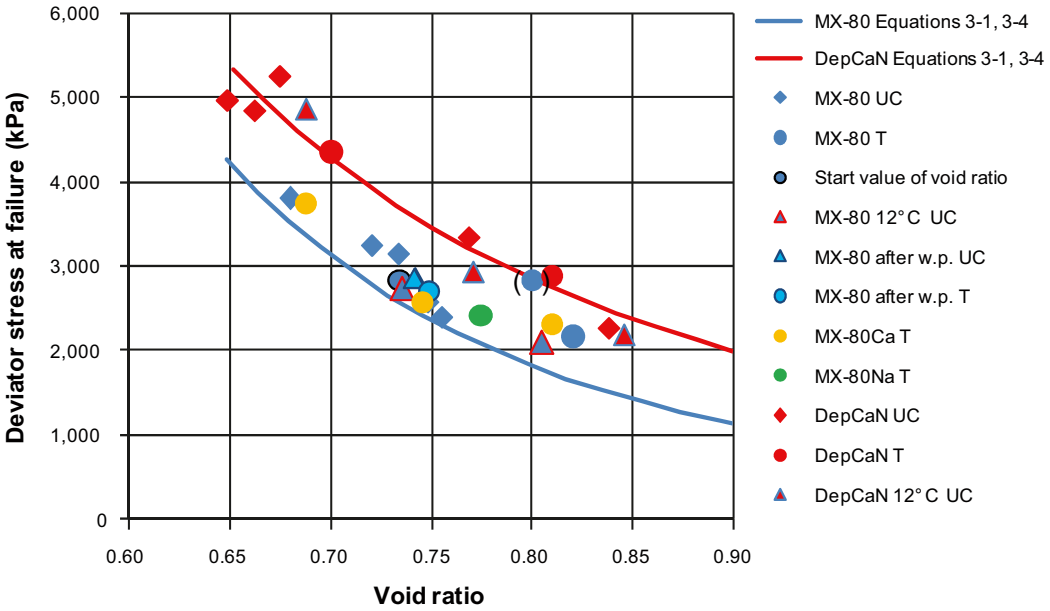

Figure 3-4. *Compilation of results from triaxial tests (market with round symbols and T) and unconfined compression tests (UC). Evaluation of Equations 3-1 and 3-4 for MX-80 and Deponit CaN is also plotted.*

3.3.3 Influence of shear rate

The shear strength that normally is measured with triaxial tests and unconfined compression tests at very low strain rates has also been measured at very high rates corresponding to the rates expected at a rock shear. Old measurements yielded the relation used in SR-Can with the rate dependence according to Equation 2-5 and the rate parameter n = 0.065. New measurements have been done on both MX-80 and Deponit CaN.

In Equation 2-5 the shear rate was formulated in absolute figures (v) and expressed in m/s. However, it is more convenient both scientifically and for the finite element modelling to instead express the rate as strain rate (v) expressed with the unity 1/s. This means that Equation 2-5 will be transformed to Equation 3-5.

$$q_{fs} = q_{fs0}\left(\frac{v_s}{v_{s0}}\right)^n \qquad (3\text{-}5)$$

where

q_{fs} = deviator stress at failure at the strain rate v_s(kPa)

q_{fs0} = deviator stress at failure at the reference strain rate v_{s0}(kPa)

v_s = strain rate (1/s)

v_{s0} = reference strain rate (1/s)

n = rate dependence factor

All results of measured shear strength are compiled in Figure 3-5 as a function of the strain rate expressed as per cent per second (%/s). Figure 3-5 shows the old results with uncoloured symbols that were the base for Equation 3-5 together with new results with coloured symbols. The dimensioning shear strength is, according to earlier conclusions, the shear strength of Deponit CaN at the density 2,050 kg/m^3. The results of a series of unconfined compression tests of that material are plotted in the figure with red filled circles. A line that follows those results is also plotted (slightly conservative as an upper limit) in the figure. Applying Equation 3-5 to that line the parameters in Equation 3-5 will have the following values:

n = 0.038

v_{s0} = 10^{-6} 1/s

q_{fs0} = 4.27 MPa

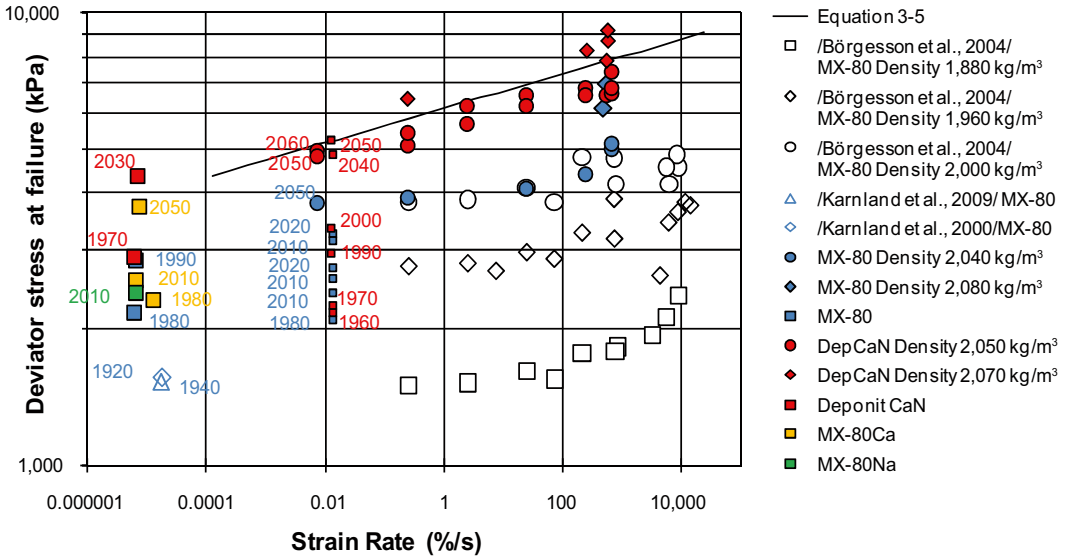

Figure 3-5. *New results (filled coloured symbols) from triaxial tests and unconfined compression tests on MX-80 plotted as function of the strain rate together with old results (uncoloured symbols) /Börgesson et al. 2004/. The dimensioning relation for Deponit CaN at the density 2,050 kg/m^3 is plotted as the straight line.*

The reference strain rate is set at $v_{s0} = 10^{-6}$ 1/s since this rate represents an average of the strain rate of the triaxial tests and the slowest unconfined compression tests and it also correspond to the strain rate of Equation 3-4 and Table 3-1 valid for Deponit CaN.

The rate dependence factor is thus lower than $n = 0.065$ that earlier was used for SR-Can. The new inclination $n = 0.038$ fits fine for the old MX-80 measurements as well. The relation is in accordance with Equations 3-1 and 3-4 at the strain rate $v = 10^{-6}$ 1/s that yielded the relation for Deponit CaN shown in Figure 3-4.

Figure 3-5 also shows that:

- The corresponding results for Deponit CaN at the density 2,070 kg/m^3 are logically located above the reference line and seem to have the same inclination.
- The inclination seems to decrease at very low strain rates since the difference between the unconfined compression test results at the strain rate 0.01%/s and the triaxial test results at the strain rate 0.00001%/s is small but this can also depend on the difference in test technique.
- The new results for MX-80 at the density 2,040 kg/m^3 are located surprisingly close to the old ones for the density 2,000 kg/m^3. The reason for this is not clear.

It is concluded that for the SR-Site calculations Equation 3-5 with the parameter values derived from the line in Figure 3-5 shall be used as dimensioning values of the shear strength of MX-80 that has been ion exchanged to Ca at the density 2,050 kg/m^3. The rate dependence is given by $n = 0.038$ and the normalizing shear strength at the strain rate $v_{s0} = 10^{-6}$ 1/s is $q_{fs0} = 4.27$ MPa. For other densities the reference strength q_{fs0} is calculated according to Equations 3-1 and 3-4 for Deponit CaN.

3.3.4 Stress-strain relation

The shape of the stress-strain relation up to failure is very similar in all type of tests and for all bentonites. Figure 3-6 shows example of four tests with different density, bentonite type, rate of deformation and test type. See also /Dueck et al. 2010/ where the stress-strain relation in all new tests is plotted.

Common for all tests is that the deviator stress increases rather fast to about half the maximum value and then starts to yield and reaches a maximum value after 3–10% strain. The small kink that often occurs at the very beginning of the test is caused by irregularities on the end surfaces of the test specimen. The behaviour after failure i.e. after maximum deviator stress may differ in the sense that some samples have a rather abrupt failure with decreasing stress after failure. However, most tests show long deformations with only very small decrease in stress i.e. an almost ideally plastic behaviour. A trend, although not generally valid, is that the strain at failure seems to decrease with increasing density and increasing Ca-content in the exchangeable ion position.

Based on the observations given above the stress-strain relation in the material model is given the following behaviour (also shown in Figure 3-7):

- Linear elastic between the strain $0 < \varepsilon < 1\%$ with an elasticity that yields 58% of the maximum Mises stress at the strain $\varepsilon = 1\%$ (blue line in Figure 3-7).
- Plastic hardening between the strain $1\% < \varepsilon < 5.3\%$ with the maximum Mises stress determined according to Section 3.3.3 (green line in Figure 3-7).
- Almost ideally plastic at $\varepsilon > 5.3\%$ (red line in Figure 3-7).

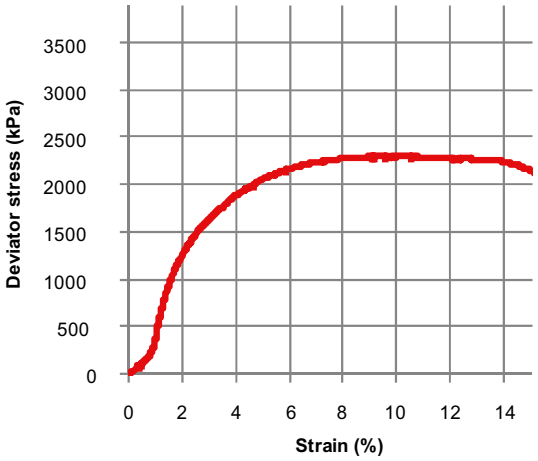

MX-80Ca, ρ = 1,990 kg/m^3, v = 1·10^{-7} m/s, triaxial test.

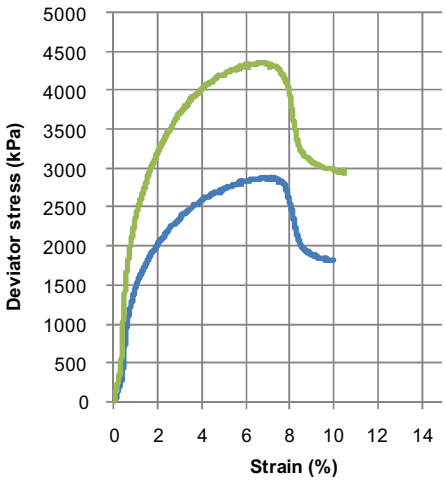

Deponit CaN, ρ = 2,030 kg/m^3 and ρ = 1,970 kg/m^3, v = 4·10^{-8} m/s, triaxial tests.

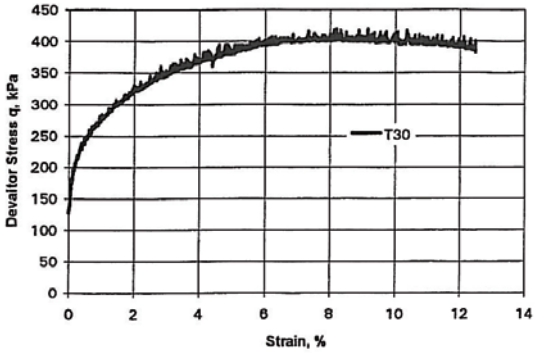

MX-80, ρ = 1,750 kg/m^3, v = 1·10^{-8} m/s, passive triaxial test.

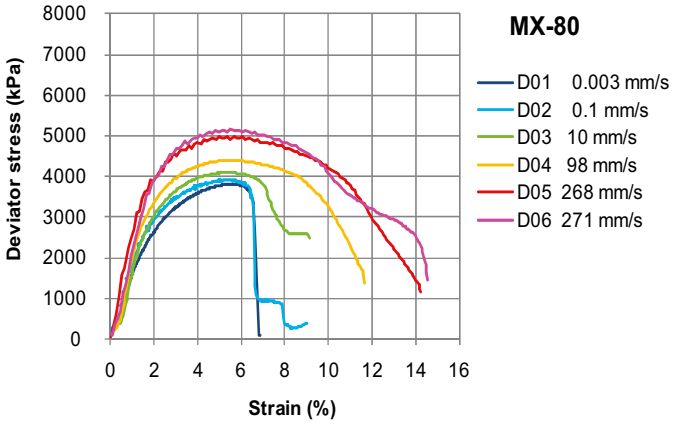

MX-80, ρ = 2,030 kg/m^3, different shear rates, unconfined compression tests.

Figure 3-6. *Examples of stress-strain relations during shear for different materials, test techniques, densities and shear rates.*

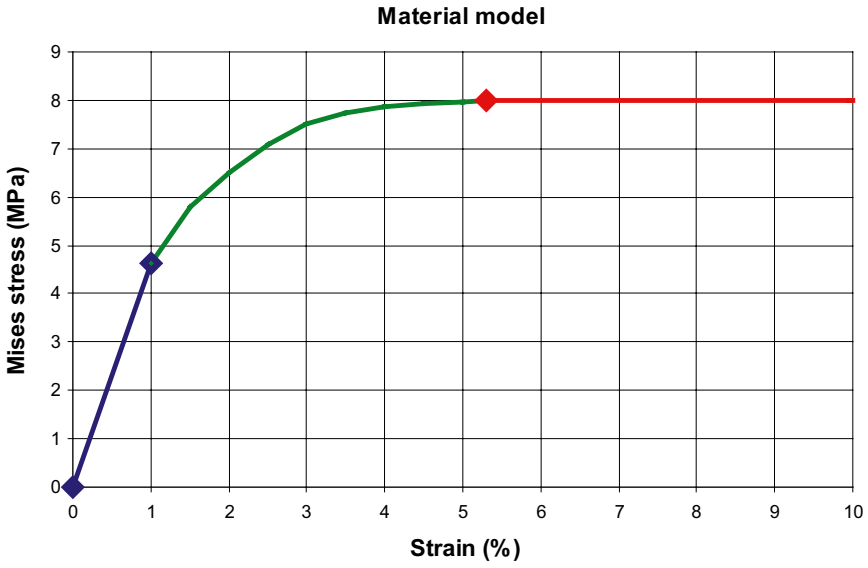

Figure 3-7. *Stress-strain relation used for the material model. Example that refers to the density 2,050 kg/m^3 at the strain rate 10 s^{-1}.*

4 Material model for SR-Site

The material model of the buffer bentonite for SR-Site is thus according to Chapter 3 a stress-strain relation that has the properties of Depoint CaN and is a function of the strain rate at unconfined compression during constant volume. The model is different at different density.

- The swelling pressure at a certain density (or void ratio) can be calculated according to Equation 3-1 with the parameters given for Deponit CaN
- The Mises stress at failure can for the strain rate $v_s = 10^{-6}$ 1/s be calculated according to Equation 3-4 with parameters for Deponit CaN given in Table 3-1
- The influence of rate of strain can be calculated according to Equation 3-5 with the parameters given for Deponit CaN.

The normalising Mises stress at failure q_{fs0} at the strain rate $v_s = 10^{-6}$ 1/s evaluated according to chapter 3 is shown for different densities in Table 4-1.

The very small differences between the calculated values of q_{fs0} and the used values in the models are caused by a small mismatch between Equations 3-4 and 3-5. The parameter q_{fs0} in Equation 3-5 for the density 2,050 kg/m^3 was originally derived from Figure 3-5 and used without considering Equation 3-4. However, since the deviation between the values used and the values derived from Equation 3-4 are very small no adjustment was considered necessary.

Based on Equation 3-5 and the relations between density, swelling pressure and strength according to Table 4-1 the new material models for Abaqus are suggested to be as described in Tables 4-2 to 4-4 with elastic and plastic properties made a function of the strain rate at different densities. Figure 4-1 shows the corresponding stress-strain relation at different strain rates for the densities 2,050 and 2,000 kg/m^3. Note that for the Abaqus analyses Young's modulus must be independent of strain rate and for density 2,050 kg/m^3 the value 462 MPa and for density 2,000 kg/m^3 the value 347 MPa were chosen /Hernelind 2010/. Previous analyses have shown that changing Young's modulus has a rather minor effect on the results.

Table 4-1. Relation between density, void ratio, swelling pressure and strength at the shear rate $v_s = 10^{-6}$ 1/s for the reference material (Deponit CaN) and the values used in the models.

ρ_m	e	p	q_{fs} (Equation 3-4)	Value of q_{fs0} used in the model
2,050 kg/m^3	0.70	12.5 MPa	4.27 MPa	4.34 MPa
2,000 kg/m^3	0.78	8.17 MPa	3.07 MPa	3.15 MPa
1,950 kg/m^3	0.87	5.32 MPa	2.21 MPa	2.29 MPa

Table 4-2. Reference bentonite model (Deponit CaN) at the density 2,050 kg/m³.

Material	ρ_m kg/m³	Rate of strain	Elastic part		Plastic part: von Mises true stress σ_j (MPa) at the following plastic nominell strains ε_p							
		v_s	E MPa	v	ε_p=0	ε_p=0.004	ε_p=0.01	ε_p=0.018	ε_p=0.026	ε_p=0.036	ε_p=0.46	ε_p=1.0
MX-80Ca	2,050	10^{-6}	251	0.49	2.51	3.35	3.85	4.11	4.27	4.34	4.29	4.29
MX-80Ca	2,050	10^{-4}	299	0.49	2.99	3.99	4.58	4.89	5.09	5.17	5.11	5.11
MX-80Ca	2,050	10^{-3}	326	0.49	3.26	4.35	5.00	5.34	5.56	5.64	5.58	5.58
MX-80Ca	2,050	10^{-2}	355	0.49	3.55	4.74	5.45	5.82	6.06	6.15	6.08	6.08
MX-80Ca	2,050	10^{-1}	388	0.49	3.88	5.18	5.95	6.36	6.62	6.72	6.65	6.65
MX-80Ca	2,050	1.0	424	0.49	4.24	5.65	6.49	6.93	7.22	7.33	7.25	7.25
MX-80Ca	2,050	10	462	0.49	4.62	6.17	7.09	7.57	7.88	8.00	7.91	7.91
MX-80Ca	2,050	100	505	0.49	5.05	6.73	7.73	8.25	8.60	8.73	8.63	8.63
MX-80Ca	2,050	1,000	551	0.49	5.51	7.35	8.44	9.02	9.39	9.53	9.43	9.43

Table 4-3. Reference bentonite model (Deponit CaN) at the density 2,000 kg/m³.

Material	ρ_m kg/m³	Rate of strain	Elastic part		Plastic part: von Mises true stress σ_j (MPa) at the following plastic nominell strains ε_p							
		v_s	E MPa	v	ε_p=0	ε_p=0.004	ε_p=0.01	ε_p=0.018	ε_p=0.026	ε_p=0.036	ε_p=0.46	ε_p=1.0
MX-80Ca	2,000	10^{-6}	182	0.49	1.82	2.43	2.79	2.98	3.10	3.15	3.11	3.11
MX-80Ca	2,000	10^{-4}	217	0.49	2.17	2.89	3.33	3.55	3.69	3.75	3.70	3.70
MX-80Ca	2,000	10^{-3}	237	0.49	2.37	3.15	3.63	3.88	4.03	4.09	4.05	4.05
MX-80Ca	2,000	10^{-2}	257	0.49	2.57	3.44	3.95	4.22	4.40	4.46	4.41	4.41
MX-80Ca	2,000	10^{-1}	281	0.49	2.81	3.76	4.31	4.61	4.80	4.87	4.82	4.82
MX-80Ca	2,000	1.0	307	0.49	3.07	4.10	4.71	5.03	5.24	5.32	5.26	5.26
MX-80Ca	2,000	10	335	0.49	3.35	4.48	5.14	5.49	5.71	5.80	5.73	5.73
MX-80Ca	2,000	100	366	0.49	3.66	4.88	5.61	5.98	6.24	6.33	6.25	6.25
MX-80Ca	2,000	1,000	399	0.49	3.99	5.33	6.12	6.54	6.81	6.91	6.83	6.83

Table 4-4. Reference bentonite model (Deponit CaN) at the density 1,950 kg/m³.

Material	ρ_m kg/m³	Rate of strain	Elastic part		Plastic part: von Mises true stress σ_j (MPa) at the following plastic nominell strains ε_p							
		v_s	E MPa	v	ε_p=0	ε_p=0.004	ε_p=0.01	ε_p=0.018	ε_p=0.026	ε_p=0.036	ε_p=0.46	ε_p=1.0
MX-80Ca	1,950	10^{-6}	132	0.49	1.32	1.76	2.03	2.16	2.24	2.29	2.25	225
MX-80Ca	1,950	10^{-4}	157	0.49	1.57	2.09	2.41	2.57	2.67	2.72	2.68	2.68
MX-80Ca	1,950	10^{-3}	172	0.49	1.72	2.28	2.63	2.81	2.92	2.96	2.93	2.93
MX-80Ca	1,950	10^{-2}	186	0.49	1.86	2.49	2.86	3.06	3.19	3.23	3.19	3.19
MX-80Ca	1,950	10^{-1}	204	0.49	2.04	2.72	3.12	3.34	3.48	3.53	3.49	3.49
MX-80Ca	1,950	1.0	223	0.49	2.23	2.97	3.41	3.64	3.79	3.85	3.81	3.81
MX-80Ca	1,950	10	243	0.49	2.43	3.24	3.72	3.98	4.14	4.20	4.15	4.15
MX-80Ca	1,950	100	265	0.49	2.65	3.54	4.06	4.33	4.52	4.59	4.53	4.53
MX-80Ca	1,950	1,000	289	0.49	2.89	3.86	4.43	4.74	4.93	5.01	4.95	4.95

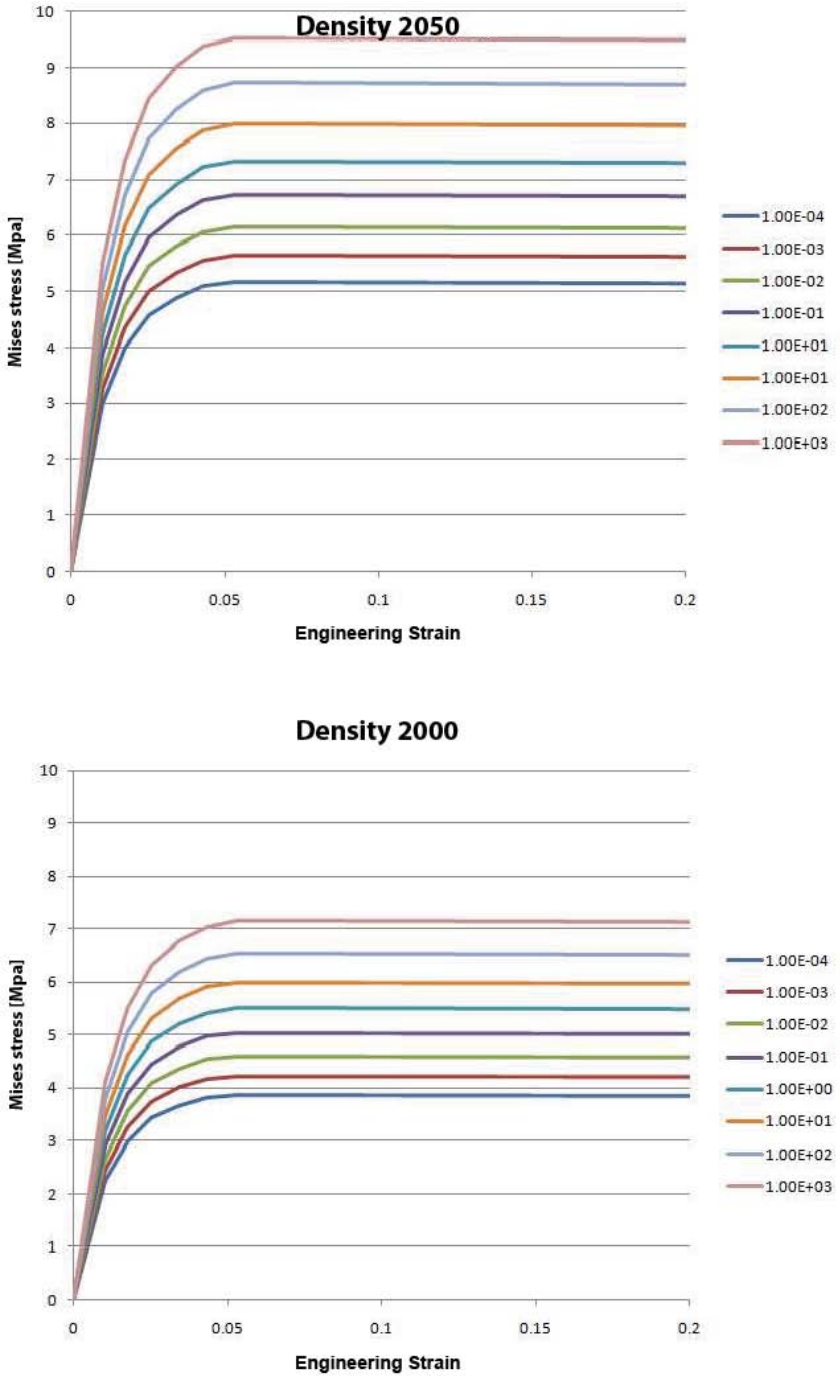

Figure 4-1. *Proposed stress-strain relations for the reference bentonite (Deponit CaN) at different strain rates and densities.*

5 Comments and conclusions

The material models described in Tables 4-2 to 4-4 and illustrated in Figure 4-1 that will be used in SR-Site are derived from a number of laboratory tests and a general understanding of the behaviour of bentonite. The bentonite is modeled as elastic-plastic with a maximum Mises stress that is rate dependant and Poisson's ratio that is close to 0.5 yielding no volume change during shear. However, the results and the evaluation of the laboratory tests are impaired by scatter and uncertainties, and as described in the previous chapters the models refer to the behaviour of the Ca-bentonite Deponit CaN. Tests made on MX-80 ion-exchanged from Na to Ca (MX-80Ca) show that the Mises stress at failure is slightly lower than for Deponit CaN. However, there are very few results for MX-80Ca (due to the time consuming and complicated procedure for ion-exchange) and no results at high shear rates so the conservative choice was to use Deponit-CaN as reference clay.

The model is a considerable improvement compared to the model used for SR-Can in the following way:

- The bentonite Deponit CaN is used as reference material. Deponit CaN is more like MX-80Ca regarding stress-strain properties and has a much lower strength than Moosburg that was used as reference Ca-bentonite in SR-Can
- The rate dependence is more realistic and reduced from about 16% to 9% increased strength for 10 times increased strain rate
- A rate dependant value of the maximum Mises stress is introduced, which reduces the stiffness in large parts of the buffer during a shear compared to the old model in SR-Can that used a constant value derived at a very high shear rate.

Tests of the influence of different factors like salt content in the ground water, history of very high water pressure and lower temperature have shown that their influence on the stress-stain properties are insignificant.

The overall conclusion is thus that a material model of the reference material is derived and well motivated and probably slightly conservative.

6 References

SKB's (Svensk Kärnbränslehantering AB) publications can be found at www.skb.se/publications.

Börgesson L, Hernelind J, 2006. Earthquake induced rock shear through a deposition hole. Influence of shear plane inclination and location as well as buffer properties on the damage caused to the canister. SKB TR-06-43, Svensk Kärnbränslehantering AB.

Börgesson L, Hernelind J, 2010. Earthquake induced rock shear through a deposition hole. Modelling of three model tests scaled 1:10. Verification of the bentonite material model and the calculation technique. SKB TR-10-33, Svensk Kärnbränslehantering AB.

Börgesson L, Johannesson L-E, Sandén T, Hernelind J, 1995. Modelling of the physical behaviour of water saturated clay barriers. Laboratory tests, material models and finite element application. SKB TR 95-20, Svensk Kärnbränslehantering AB.

Börgesson L, Johannesson L-E, Hernelind J, 2004. Earthquake induced rock shear through a deposition hole. Effect on the canister and the buffer. SKB TR-04-02, Svensk Kärnbränslehantering AB.

Dueck A, Börgesson L, Johannesson L-E, 2010. Stress-strain relation of bentonite at undrained shear. Laboratory tests to investigate the influence of material composition and test technique. SKB TR-10-32, Svensk Kärnbränslehantering AB.

Harrington J F, Birchall D J, 2007. Sensitivity of total stress to changes in externally applied water pressure in KBS-3 buffer bentonite. SKB TR-06-38, Svensk Kärnbränslehantering AB.

Hernelind J, 2010. Modelling and analysis of canister and buffer for earthquake induced rock shear and glacial load. SKB TR-10-34, Svensk Kärnbränslehantering AB.

Raiko H, Sandström R, Rydén H, Johansson M, 2010. Design analysis report for the canister. SKB TR-10-28, Svensk Kärnbränslehantering AB.